Appendix A.45:

St. Albans Catholic School – VsVp 57180

Table 1: Site Description for St. Albans Catholic School (VsVp 57180).

Attribute	Yes/No			Description/Date	Symbol in Figure 1
	10-m Buffer	20-m Buffer	50-m Buffer		
Near a body of surface water or other free face features?	No	No	No	The center of the site is ~210 m to the NW from the unnamed stream (the free-face height is ~0.5-1 m).	NA
Lateral spreading observed during the CES?	No	No	No	No lateral spreading was observed by the mapping team.[1]	NA
Nearby buildings or structures?	Yes	Yes	Yes	Building coverage of the 10-, 20-, and 50-m buffers is 1, 14, and 26%, respectively. They are in the SW quadrant of the 10-m buffer, the SE, SW, and NW quadrants of the 20-m buffer, and all quadrants of the 50-m buffer.	White Fill + Brown Outline
Sloping land?	No	No	No	Flat land, residential area	NA
Step changes in the ground surface?	No	No	No	NA	NA
Retaining walls?	No	No	No	NA	NA
Vegetation?	Yes	Yes	Yes	Trees and bushes cover 42, 35, and 30% of the 10-, 20-, and 50-m buffers. They are in all quadrants of the buffers.	White Fill + Green Outline
Manmade changes to the site between the LiDAR surveys?	Yes	Yes	Yes	Vegetation removal in the N portion of all buffers between Jan 2007 and Mar 2009. Vegetation removal in the SW quadrant of the 50-m buffer between Aug 2011 and Apr 2012. Vegetation addition in the NE quadrant of all buffers between Apr 2012 and Oct 2012.	Vegetation Changes: Green Outline/ Crossline
Other important factors?	Yes	Yes	Yes	Moderate-motor-vehicle-volume road (Rutland St) occupies 13% of the 20- and 50-m buffers and stretches throughout the NE and SE quadrants. Unknown object in the SW quadrant of the 20- and 50-m buffers appears in Mar 2009 but is removed prior to Sep 3, 2010. Unknown object in the NE quadrant of all buffers from Feb 2011 to Oct 2012.	Road: Gray Fill + Red Outline; Unknown Object: Purple Outline

Note: Buffer is the area within a circle of a specified radius with CPT investigations done at its center (172.629117°, -43.507198°).

[1] Canterbury Geotechnical Database. (2012). "Observed Ground Crack Locations", Map Layer CGD0400 - 23 July 2012, retrieved July 09, 2018 from https://canterburygeotechnicaldatabase.projectorbit.com/

Figure 1: Site plan with areas where ejecta-induced settlement is considered.

Note 1: Patch A (outlined in red) in the free field was selected for settlement assessment as an area free of vegetation and structures. Other important factors considered for the patch selection were its proximity to a CPT, a property subjected to addition and/or demolition of a structure, front yard/backyard alterations (e.g., ploughing, rubble, scrap), and aerial distribution of sediment ejecta. The entire portion of the road within the 50-m buffer was considered for settlement assessment, too. The LiDAR-based settlement analyses of Patch A and Road were not considered for any earthquake event due to the evident absence of ejecta for the Sep-10 and Dec-11 EQs and minor quantum of ejecta for the Feb-11 and Jun-11 EQs.

Table 2: LiDAR flight error adjustments, global adjustments for the difference between average LiDAR point elevations and benchmark survey elevations, and vertical tectonic movement adjustments.

	Adjustments (mm)		
Earthquake Event(s)	LiDAR Flight Error	Global Offset[2]	Tectonic Vertical Movement
Sep-10	0	-3	0
Feb-11	0	16	-60
Jun-11	0	38	-30
Dec-11	-50	-65	0
CES	-50	-14	-90
Any LiDAR survey affected by ejecta?			No

Note: The negative sign indicates the subtraction from the ground surface subsidence, while the positive sign indicates the addition to the ground surface subsidence.

Table 3a: LiDAR Measurement Error for Patch A.

Surveys	Buffer	Area Averaged Difference Indicating Repeat Measurement Error (mm)	σ* individual LiDAR points (mm)	%Reduction in σ due to Area Averaging of LiDAR Points
Post Feb 2011: Mar 2011 and May 2011	10-m	ND	59	[ND,ND]
	20-m	ND		
	50-m	ND		
Post Dec 2011: Feb 2012 and Oct 2015	10-m	ND	70	[ND,ND]
	20-m	ND		
	50-m	ND		

*Standard deviation; ND = Not determined.

[2] Russell, J., & van Ballegooy, S. (2015). *Canterbury Earthquake Sequence: Increased liquefaction vulnerability assessment methodology*. New Zealand: Tonkin & Taylor Ltd.

Table 3b: LiDAR Measurement Error for Road.

Surveys	Buffer	Area Averaged Difference Indicating Repeat Measurement Error (mm)	$\sigma^*_{\text{individual LiDAR points}}$ (mm)	%Reduction in σ due to Area Averaging of LiDAR Points
Post Feb 2011: Mar 2011 and May 2011	10-m	NA	59	[ND,ND]
	20-m	NA		
	50-m	ND		
Post Dec 2011: Feb 2012 and Oct 2015	10-m	NA	70	[ND,ND]
	20-m	NA		
	50-m	ND		

*Standard deviation.

Table 4a: Ground surface subsidence adjustments due to LiDAR measurement error for Patch A.

Earthquake Event(s)	$\sigma_{\text{pre-EQ LiDAR survey}}$ (mm)	$\sigma_{\text{post-EQ LiDAR survey}}$ (mm)	σ_{total} (mm)	Area Average Adjusted σ (mm) **
Sep-10	158	56	134	ND
Feb-11	56	59	59	ND
Jun-11	59	61	62	ND
Dec-11	61	70	87	ND
CES	158	70	124	ND

**Based on the highest %Reduction in Table 3a.

Table 4b: Ground surface subsidence adjustments due to LiDAR measurement error for Road.

Earthquake Event(s)	$\sigma_{\text{pre-EQ LiDAR survey}}$ (mm)	$\sigma_{\text{post-EQ LiDAR survey}}$ (mm)	σ_{total} (mm)	Area Average Adjusted σ (mm) **
Sep-10	158	56	134	ND
Feb-11	56	59	59	ND
Jun-11	59	61	62	ND
Dec-11	61	70	87	ND
CES	158	70	124	ND

**Based on the highest %Reduction in Table 3b.

Table 5a: Raw liquefaction-related ground surface subsidence using original LiDAR points for Patch A.

Earthquake Event(s)	Average Ground Surface Subsidence (mm) 10-m Buffer	20-m Buffer	50-m Buffer
Sep-10	ND	ND	ND
Feb-11	ND	ND	ND
Jun-11	ND	ND	ND
Dec-11	ND	ND	ND
CES	ND	ND	ND

ND = Not determined due to the manmade changes.

Table 5b: Raw liquefaction-related ground surface subsidence using original LiDAR points for Road.

Earthquake Event(s)	Average Ground Surface Subsidence (mm) 10-m Buffer	20-m Buffer	50-m Buffer
Sep-10	NA	NA	ND
Feb-11	NA	NA	ND
Jun-11	NA	NA	ND
Dec-11	NA	NA	ND
CES	NA	NA	ND

Table 6a: Corrected liquefaction-related ground surface subsidence using original LiDAR points for Patch A with the calculated adjustments in Table 2.

Earthquake Event(s)	Average Calculated Ground Surface Subsidence (mm) 10-m Buffer	20-m Buffer	50-m Buffer
Sep-10	ND	ND	ND
Feb-11	ND	ND	ND
Jun-11	ND	ND	ND
Dec-11	ND	ND	ND
CES	ND	ND	ND

Notes: Plus/minus values are same as those in Table 4a, but rounded to the nearest 25 mm; Positive overall values indicate ground surface subsidence, while negative overall values indicate ground surface uplift; ND = Not determined.

Table 6b: Corrected liquefaction-related ground surface subsidence using original LiDAR points for Road with the calculated adjustments in Table 2.

	Average Calculated Ground Surface Subsidence (mm)		
Earthquake Event(s)	10-m Buffer	20-m Buffer	50-m Buffer
Sep-10	NA	NA	ND
Feb-11	NA	NA	ND
Jun-11	NA	NA	ND
Dec-11	NA	NA	ND
CES	NA	NA	ND

Notes: Plus/minus values are same as those in Table 4b, but rounded to the nearest 25 mm; Positive overall values indicate ground surface subsidence, while negative overall values indicate ground surface uplift.

Table 7a: Corrected liquefaction-related ground surface subsidence for Patch A using LiDAR DEMs.

	Estimated Ground Surface Subsidence (mm)								
	10-m Buffer			20-m Buffer			50-m Buffer		
Earthquake Event(s)	16th %ile	50th %ile	84th %ile	16th %ile	50th %ile	84th %ile	16th %ile	50th %ile	84th %ile
Sep-10	ND	ND	ND	ND	ND	ND	ND	ND	ND
Feb-11	<50	50	100	<50	50	100	<50	50	100
Jun-11	<50	<50	50	<50	<50	50	<50	<50	50
Dec-11	<50	<50	<50	<50	<50	<50	<50	<50	<50
CES	ND	ND	ND	ND	ND	ND	ND	ND	ND

Note: These percentiles are not the exact statistical measures; they indicate the spatial variability of ground surface subsidence; ND = Not determined.

Table 7b: Corrected liquefaction-related ground surface subsidence for Patch B using LiDAR DEMs.

	Estimated Ground Surface Subsidence (mm)								
	10-m Buffer			20-m Buffer			50-m Buffer		
Earthquake Event(s)	16th %ile	50th %ile	84th %ile	16th %ile	50th %ile	84th %ile	16th %ile	50th %ile	84th %ile
Sep-10	NA	NA	NA	NA	NA	NA	<50	<50	50
Feb-11	NA	NA	NA	NA	NA	NA	50	100	100
Jun-11	NA	NA	NA	NA	NA	NA	<50	<50	50
Dec-11	NA	NA	NA	NA	NA	NA	<50	<50	<50
CES	NA	NA	NA	NA	NA	NA	200	200	300

Note: These percentiles are not the exact statistical measures; they indicate the spatial variability of ground surface subsidence.

Table 8a: Ejecta-Induced settlement for the top 20 m of the soil profile for Patch A for the 50th %ile PGA, P_L=50%, and C_{FC}=0.13 using BI-2014, ZRB-2002, and I_C cutoff of 2.6.

Earthquake Event(s)	M_W	PGA (g)	Depth to Groundwater (m)	S_T (mm)	S_{V1D} (mm)	$S_{E,L}$ (mm)
Sep-10	7.1	0.21	1.5	ND	99±20	ND
Feb-11	6.2	0.34	1.5	ND	163±50	ND
Jun-11	6.2	0.18	0.5	ND	62±25	ND
Dec-11	6.1	0.21	1.2	ND	67±50	ND

Notes: S_T = Total settlement (Table 6); S_{V1D} = Average vertical settlement due to volumetric compression using Boulanger and Idriss (2014) (BI-2014), Zhang et al. (2002) (ZRB-2002) procedures and de Greef and Lengkeek (2018) thin-layer correction; $S_{E,L}$ = Ejecta-induced settlement as the difference between the LiDAR-based S_T and S_{V1D}; ND = Not determined.

Table 8b: Ejecta-Induced settlement for the top 20 m of the soil profile for Road for the 50th %ile PGA, P_L=50%, and C_{FC}=0.13 using BI-2014, ZRB-2002, and I_C cutoff of 2.6.

Earthquake Event(s)	M_W	PGA (g)	Depth to Groundwater (m)	S_T (mm)	S_{V1D} (mm)	$S_{E,L}$ (mm)
Sep-10	7.1	0.21	1.5	ND	69±20	ND
Feb-11	6.2	0.34	1.5	ND	126±50	ND
Jun-11	6.2	0.18	0.5	ND	40±25	ND
Dec-11	6.1	0.21	1.2	ND	43±50	ND

Notes: S_T = Total settlement (Table 6); S_{V1D} = Average vertical settlement due to volumetric compression using Boulanger and Idriss (2014) (BI-2014), Zhang et al. (2002) (ZRB-2002) procedures and de Greef and Lengkeek (2018) thin-layer correction; $S_{E,L}$ = Ejecta-induced settlement as the difference between the LiDAR-based S_T and S_{V1D}.

Note 2: The uncertainty for volumetric settlement was derived based on the sensitivity of volumetric settlement to PGA, C_{FC}, and P_L for each earthquake event for VsVp 57203 *Shirley Intermediate School* and CC LIQ 1 – CPT 5586 – *Vivian St* sites. Taking the 50th percentile as the baseline case, the minimum and maximum values corresponding to the difference between the 25th percentile and the 50th percentile and the 75th percentile and the 50th percentile were determined. The arithmetic mean of the range of the minimum and maximum difference was evaluated for each patch at the two sites. The maximum arithmetic mean for each earthquake event was rounded to the nearest five and used as the uncertainty value. Accordingly, the 1-D volumetric settlement uncertainties of ±20, ±50, ±25, and ±50 mm for the Sep-10, Feb-11, Jun-11, and Dec-11 earthquake events, respectively, were used for all sites in this study.

Table 9a: Coverage area and height of ejecta estimates for Patch A (10-m buffer) using photographs.

Earthquake Event	$A_{E,thick}$ (m^2)	$H_{E,thick}$ (mm)	$A_{E,thin}$ (m^2)	$H_{E,thin}$ (mm)	A_T (m^2)
Sep-10	0	0	0	0	129
Feb-11	9.68	30-50	0	0	129
Jun-11	5.8	20-40	0	0	113
Dec-11	0	0	0	0	129

Notes: $A_{E,thick/thin}$ = Coverage area of thick/thin ejecta layers; $H_{E,thick/thin}$ = Lower-upper estimate of height of thick/thin ejecta layers; A_T = Total assessment area of a buffer being considered; Thin and thick layers correspond to light gray and dark gray colors of ejecta observed in aerial photographs.

Table 9b: Coverage area and height of ejecta estimates for Patch A (20-m and 50-m buffers) using photographs.

Earthquake Event	$A_{E,thick}$ (m^2)	$H_{E,thick}$ (mm)	$A_{E,thin}$ (m^2)	$H_{E,thin}$ (mm)	A_T (m^2)
Sep-10	0	0	0	0	168
Feb-11	19.2	30-50	0	0	168
Jun-11	13.3	20-40	0	0	168
Dec-11	0	0	0	0	168

Notes: $A_{E,thick/thin}$ = Coverage area of thick/thin ejecta layers; $H_{E,thick/thin}$ = Lower-upper estimate of height of thick/thin ejecta layers; A_T = Total assessment area of a buffer being considered; Thin and thick layers correspond to light gray and dark gray colors of ejecta observed in aerial photographs.

Table 9c: Coverage area and height of ejecta estimates for Road (50-m buffer) using photographs.

EQ Event	H_{E,c_thin} (mm)	A_{E,c_thin} (m^2)	H_{E,c_thick}/ $H_{E,cc}$** (mm)	A_{E,c_thick} (m^2)/ $V_{E,cc}$** (m^3)	$H_{E,prism}$ (mm)	$V_{E,prism}$ (m^3)	$H_{E,thin/thick}$ (mm)	$A_{E,thin/thick}$ (m^2)	A_T (m^2)
Sep-10	0	0	0	0	0	0	0	0	1027
Feb-11	60-120	2.27	80-160	6.6	7-31	0.17-0.34	2-4/5-10	6.7/433	950*
Jun-11	0	0	358-826	3.82	31-104	0.91-1.81	1-2	857	916*
Dec-11	0	0	0	0	0	0	0	0	1027

Notes: $H_{E,c\_thin/thick}$ = Lower-upper estimate of height of thin/thick conically shaped ejecta layers; $A_{E,c\_thin/thick}$ = Coverage area of thin/thick conically shaped ejecta layers for the Feb-11 EQ; A_T = Total assessment area of a buffer being considered; Thin and thick layers correspond to light gray and dark gray colors of ejecta observed in aerial photographs; * indicates the reduction in A_T due to the presence of objects (e.g., cars); $A_{E,thin/thick}$ = Coverage area of thin/thick ejecta layers; * indicates uncertainty due to the place of origin; $H_{E,\ thin/thick}$ = Lower-upper estimate of height of thin/thick ejecta layers; $H_{E,prism}$ = Lower-upper estimate of ejecta height near the curb based on 2-4% cross slope of normal crown; $V_{E,prism}$ = Lower-upper estimate of total volume of prismatic-shape ejecta; $H_{E,cc}$ and $V_{E,cc}$ are the height and volume, respectively, of ejecta piles shaped as a cone with the repose angle of 30° for the Jun-11 EQ.

Note 3: The values in Table 9 correspond to the coverage area of ejecta outlined in aerial photographs (Figures 38 and 39) and the lower and upper estimates of ejecta height based on geometrical approximations and EQC LDAT property inspection reports. The ejecta-induced settlement using photographs and engineering judgment, $S_{E,P}$, is estimated as

$$S_{E,P} = \frac{\sum_{i=1}^{a} A_{E,thick,i} * H_{E,thick,i} + \sum_{j=1}^{b} A_{E,thin,j} * H_{E,thin,j} + \frac{1}{3}\sum_{k=1}^{c} A_{E,pile,k} * R_{E,pile,k} * tan30°}{A_T} + \frac{\frac{1}{3}\sum_{m=1}^{e} A_{E,cone,m} * H_{E,cone,m} + \frac{1}{2}\sum_{n=1}^{f} W_{E,prism,n} * H_{E,prism,n} * L_{E,prism,n}}{A_T}$$

$$= \frac{\sum_{i=1}^{a} V_{E,thick,i} + \sum_{j=1}^{b} V_{E,thin,j} + \sum_{k=1}^{c} V_{E,conical\ component,k}}{A_T} + \frac{\sum_{m=1}^{e} V_{E,cone,m} + \sum_{n=1}^{f} V_{E,prism,n}}{A_T}$$

where

- $A_{E,thick,i}$ and $H_{E,thick,i}$ are the area and the height of a thick ejecta layer, respectively;
- $A_{E,thin,j}$ and $H_{E,thin,j}$ are the area and the height of a thin ejecta layer, respectively;
- $A_{E,pile,k}$ and $R_{E,pile,k}$ are the area and the radius of an ejecta pile component, respectively, shaped as a cone with the repose angle of 30°;
- $A_{E,cone,m}$ and $H_{E,cone,m}$ are the area and the height of a conically shaped ejecta, respectively;
- $W_{E,prism,n}$ and $L_{E,prism,n}$ are the width and the length of the coverage area of a prismatically shaped ejecta layer, respectively, and $H_{E,prism,n}$ is the height of a prism-like ejecta layer;
- A_T is the total assessment area for a buffer being considered (Figure 1).

Table 10: Ejecta-induced settlement estimates for Patch A and Road based on photographs.

Earthquake Event	Patch A (10-m buffer)		Patch A (20- and 50-m buffers)		Road (50-m buffer)	
	$S_{E,P,lower}$ (mm)	$S_{E,P,upper}$ (mm)	$S_{E,P,lower}$ (mm)	$S_{E,P,upper}$ (mm)	$S_{E,P,lower}$ (mm)	$S_{E,P,upper}$ (mm)
Sep-10	0	0	0	0	0	0
Feb-11	2	4	3	6	1	3
Jun-11	1	2	2	3	2-6	4-8
Dec-11	0	0	0	0	0	0

Note: $S_{E,P,lower}$ and $S_{E,P,upper}$ correspond to lower and upper estimates of $S_{E,P}$, respectively.

Table 11: Best final estimates of ejecta-induced settlement for Patch A and Road.

EQ Event	Patch A (10-m buffer)			Patch A (20- and 50-m buffers)			Road (50-m buffer)		
	$S_{E,L}$ (mm)	$S_{E,P}$ (mm)	$S_{E,final}$ (mm)	$S_{E,L}$ (mm)	$S_{E,P}$ (mm)	$S_{E,final}$ (mm)	$S_{E,L}$ (mm)	$S_{E,P}$ (mm)	$S_{E,final}$ (mm)
Sep-10	ND	0	0	ND	0	0	ND	0	0
Feb-11	ND	3±1	5±5	ND	4.5±1.5	5±5	ND	2±1	<5
Jun-11	ND	1.5±0.5	<5	ND	2±1	<5	ND	5±3	5±5
Dec-11	ND	0	0	ND	0	0	ND	0	0

Notes: $S_{E,L}$ = Ejecta-induced settlement based on LiDAR data reported in Table 8; $S_{E,P}$ = Median ejecta-induced settlement for the range of values reported in Table 10; $S_{E,final}$ = Best final estimate of ejecta-induced settlement rounded to the nearest 5 mm; Final plus/minus values are also rounded to the nearest 5 mm; ND = Not determined.

Note 4:

- $S_{E,final}$ for Patch A and Road is based solely on $S_{E,P}$ for all earthquake events due to the evidence of no ejecta or minor ejecta.
- The St. Albans Catholic School site is not in the apparent zone of higher or lower ground surface subsidence for the Sep-10 or Feb-11 EQ. The site is in the zone of moderate LPI overprediction of liquefaction severity for the Sep-10 EQ and slight to moderate LPI overprediction of liquefaction severity for the Feb-11 EQ (Maurer et al. 2014[3]). The LDAT property inspection reports are available for nearby properties; the ejecta height was noted as <100 mm and <200 mm in May 2011. There are no ground photographs of Patch A and Road.

<u>Summary</u>:

- **The best estimate of the ejecta-induced free-field ground settlement at the St. Albans Catholic School site for the SEP 2010, FEB 2011, JUN 2011, and DEC 2011 earthquake is 0 mm, 5±5 mm, <5 mm, and 0 mm, respectively.**
- **The best estimate of the ejecta-induced free-field ground settlement of the road at the St. Albans Catholic School site for the SEP 2010, FEB 2011, JUN 2011, and DEC 2011 earthquake is 0 mm, <5 mm, 5±5 mm, and 0 mm, respectively.**

[3] Maurer, B. W., Green, R. A., Cubrinovski, M., & Bradley, B. A. (2014). Evaluation of the Liquefaction Potential Index for Assessing Liquefaction Hazard in Christchurch, New Zealand. *Journal of Geotechnical and Geoenvironmental Engineering*, 140(7), 04014032-1-11. doi:10.1061/(asce)gt.1943-5606.0001117

Figure 2: Location of the site.

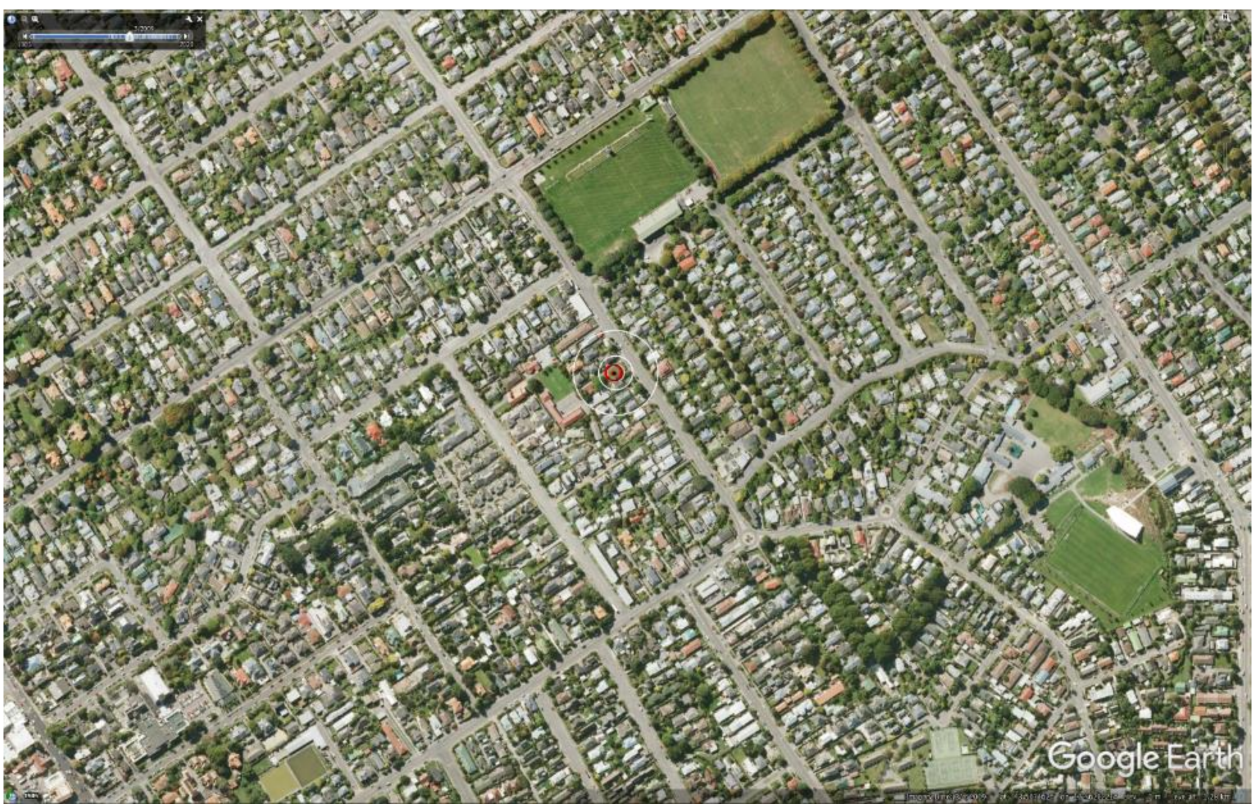

Figure 3: Position of the site relative to nearby buildings, vegetation, and free-face features.

Figure 4: Street view of the flat land.

Figure 5: Satellite image of the site taken in Dec 2004.

Figure 6: Satellite image of the site taken in Jan 2007.

Figure 7: Satellite image of the site taken in Mar 2009.

Figure 8: Satellite image of the site taken on Sep 3, 2010.

Figure 9: Satellite image of the site taken on Sep 5, 2010.

Figure 10: Satellite image of the site taken on Feb 7, 2011.

Figure 11: Satellite image of the site taken on Feb 23, 2011.

Figure 12: Satellite image of the site taken on Feb 26, 2011.

Figure 13: Satellite image of the site taken on Mar 28, 2011.

Figure 14: Satellite image of the site taken on Aug 30, 2011.

Figure 15: Satellite image of the site taken in Apr 2012.

Figure 16: Satellite image of the site taken in Oct 2012.

Figure 17: Satellite image of the site taken in Nov 2015.

Figure 18: Aerial photograph of the site taken on Sep 4, 2010.

Figure 19: Aerial photograph of the site taken on Feb 24, 2011.

Figure 20: Aerial photograph of the site taken on June 14-15, 2011.

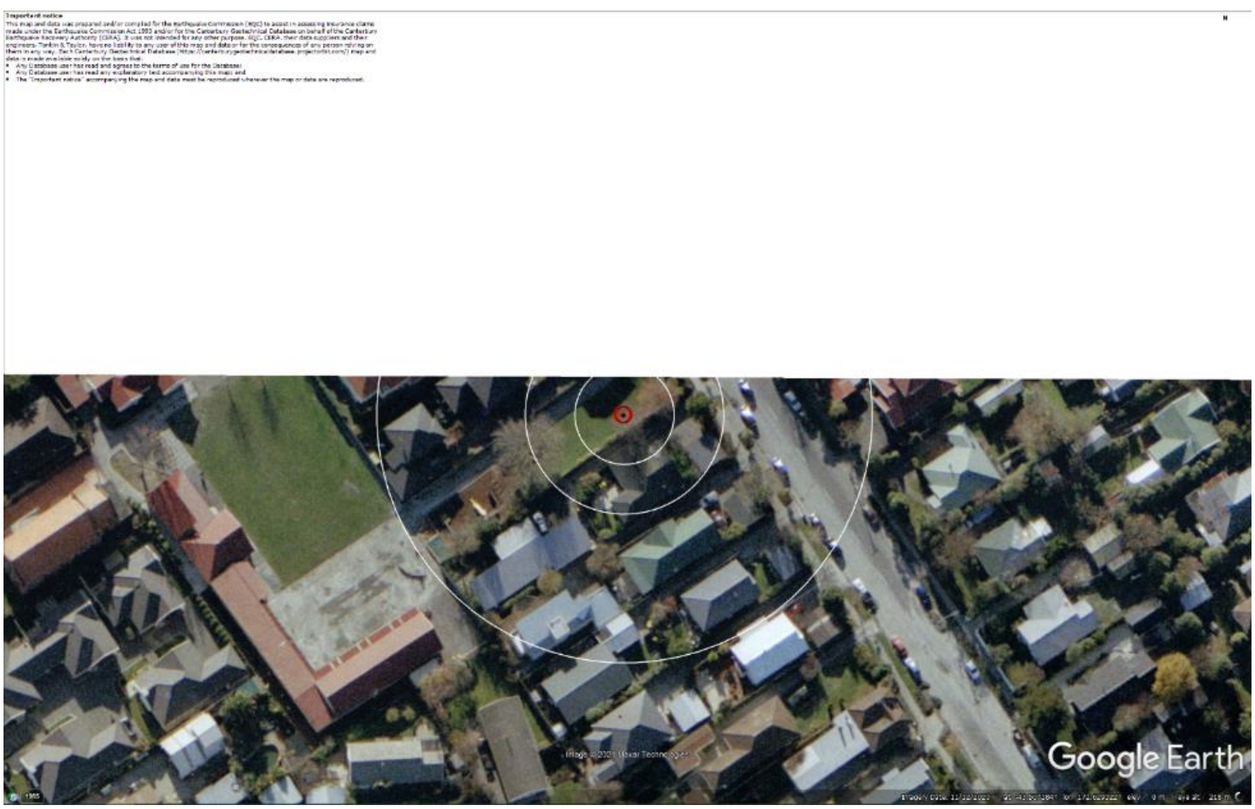

Figure 21: Aerial photograph of the site taken on June 16, 2011.

Figure 22: Aerial photograph of the site taken on Dec 24, 2011.

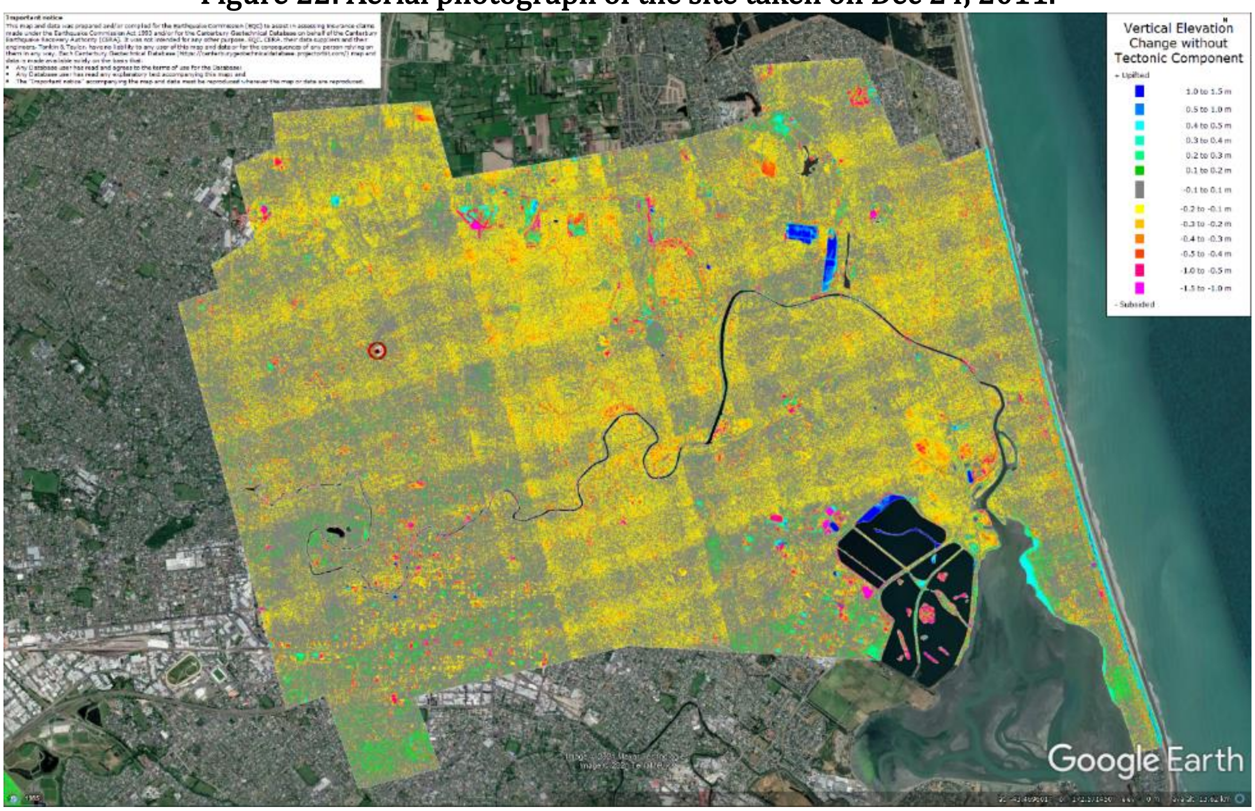

Figure 23: Vertical Ground Movements (Surface – Tectonic) for Sep 2010 Earthquake – the site is not in the apparent zone of overestimated ground surface subsidence.

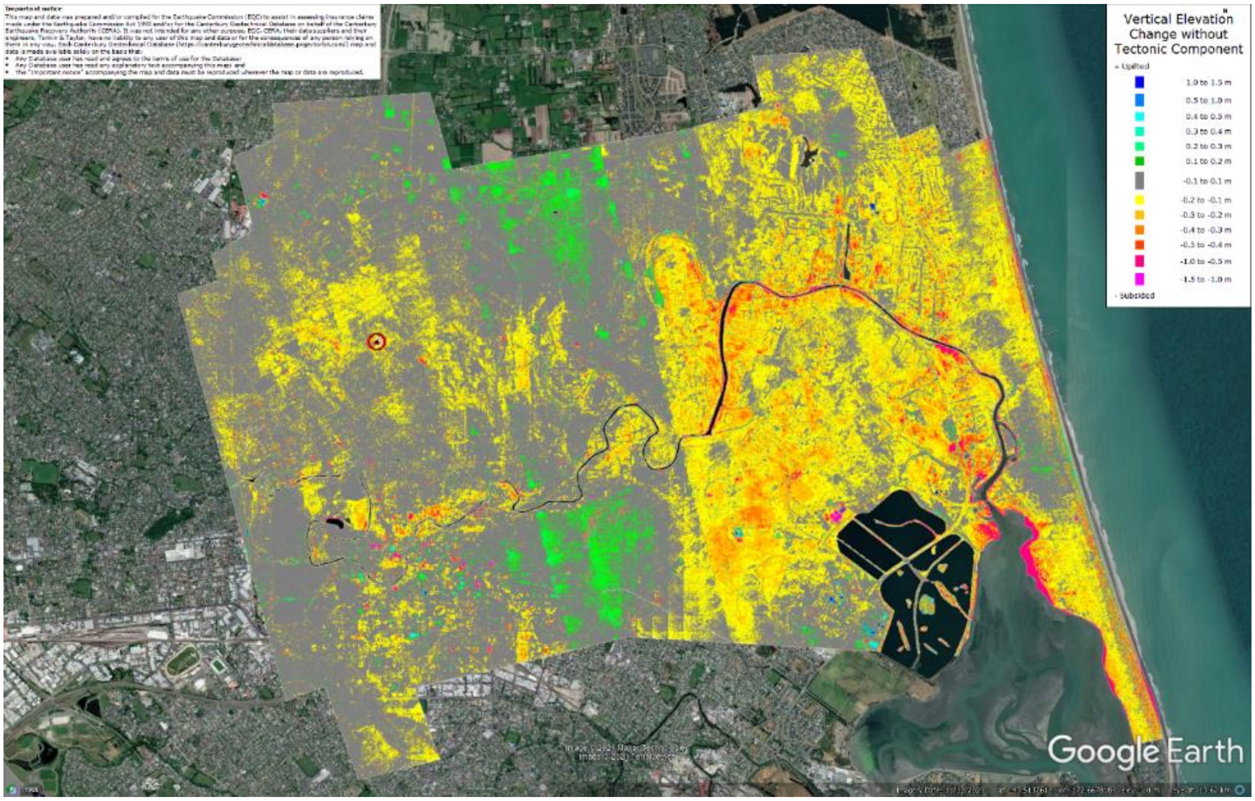

Figure 24: Vertical Ground Movements (Surface – Tectonic) for Feb 2011 Earthquake – the site is not in the apparent zone of underestimated ground surface subsidence.

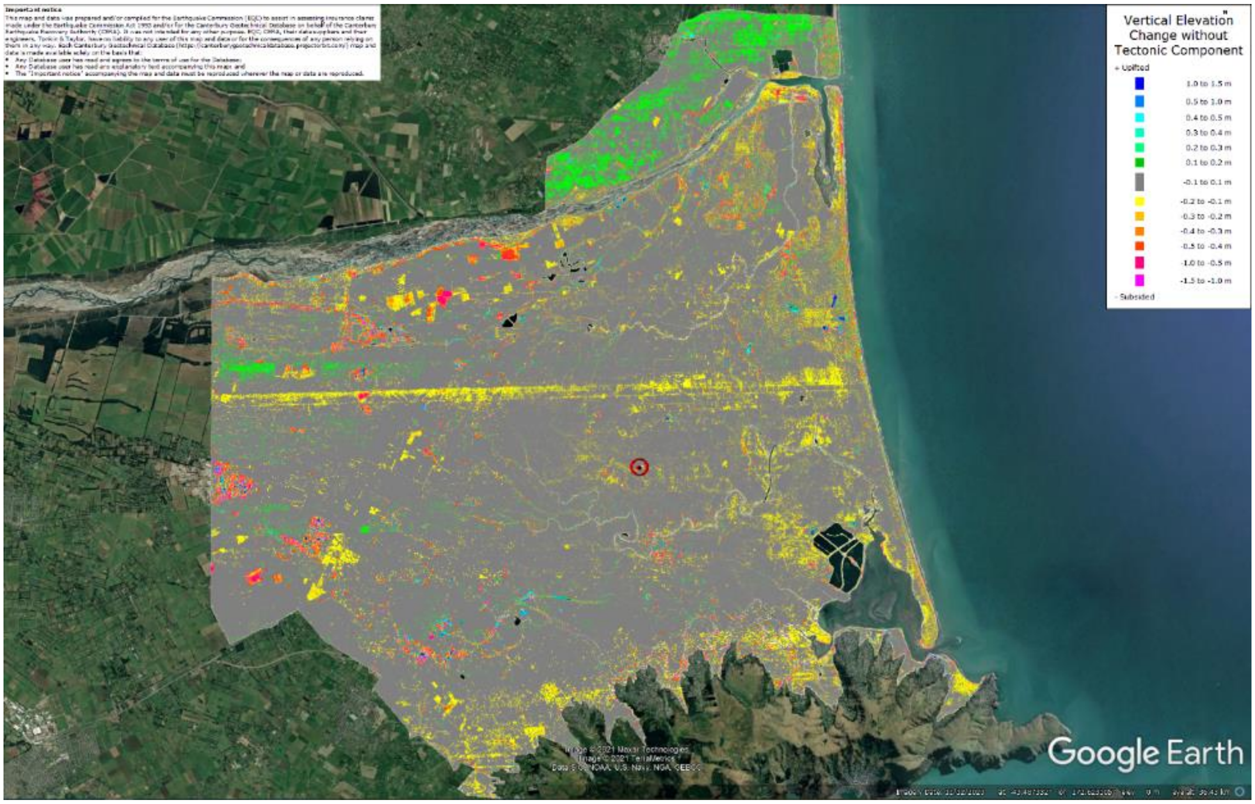

Figure 25: Vertical Ground Movements (Surface – Tectonic) for June 2011 Earthquake – the site is not in the apparent zone of overestimated or underestimated ground surface subsidence.

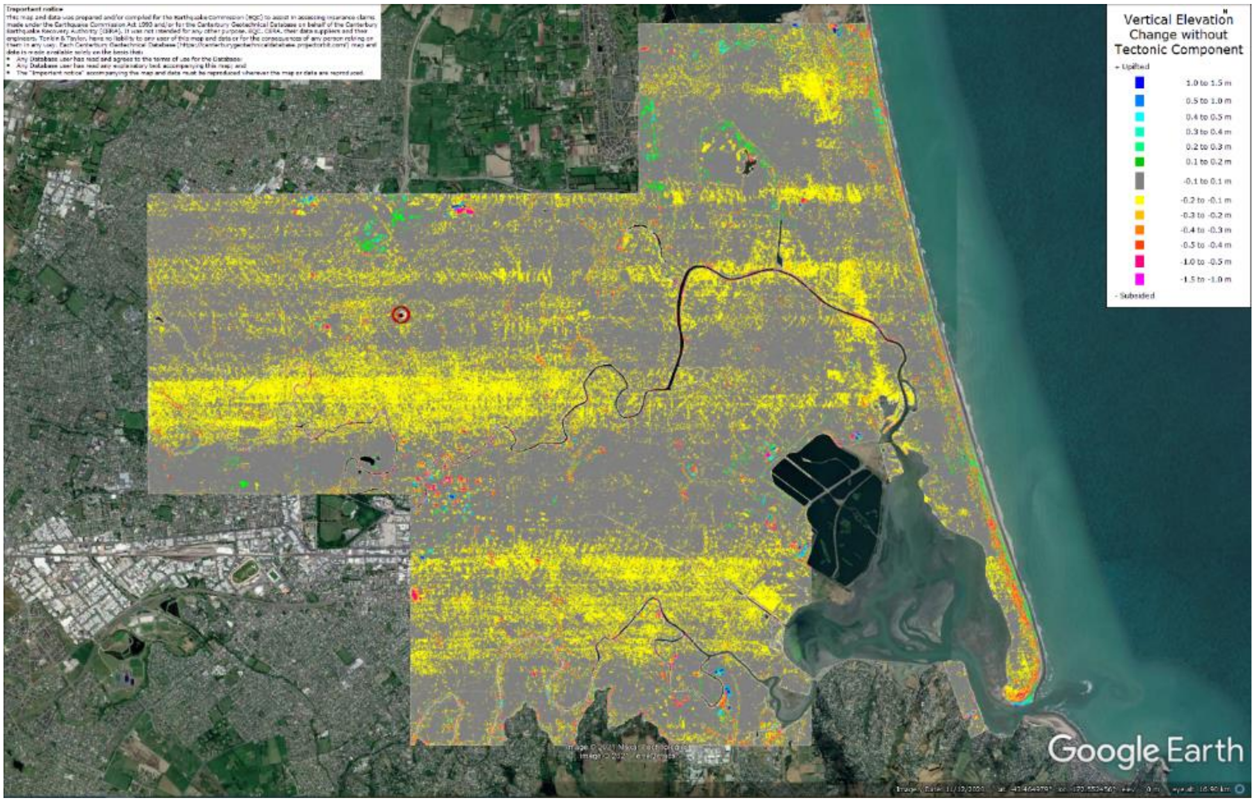

Figure 26: Vertical Ground Movements (Surface – Tectonic) for Dec 2011 Earthquake – the site is in the apparent zone of overestimated ground surface subsidence (i.e., Feb 2012 LiDAR flight band error).

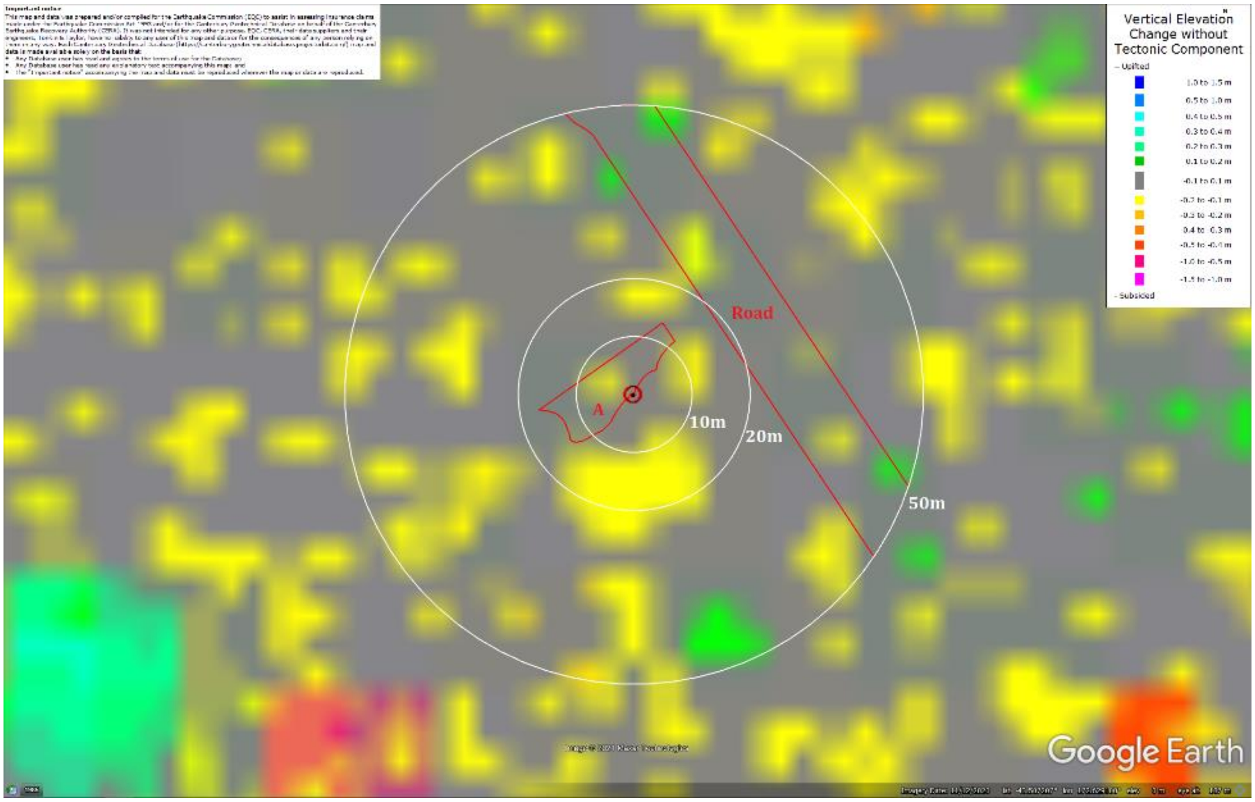

Figure 27: Ground surface subsidence without tectonic component for Sep 2010 Earthquake according to the LiDAR DEM.

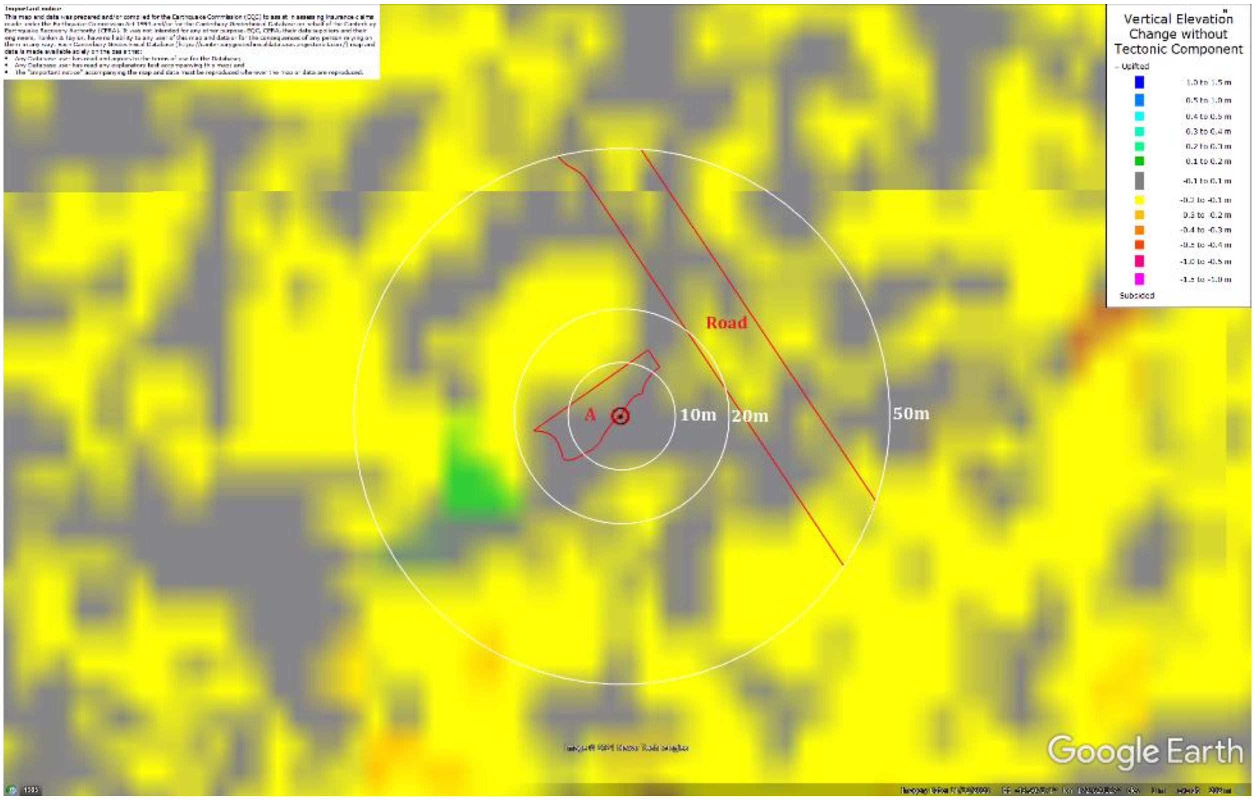

Figure 28: Ground surface subsidence without tectonic component for Feb 2011 Earthquake according to the LiDAR DEM.

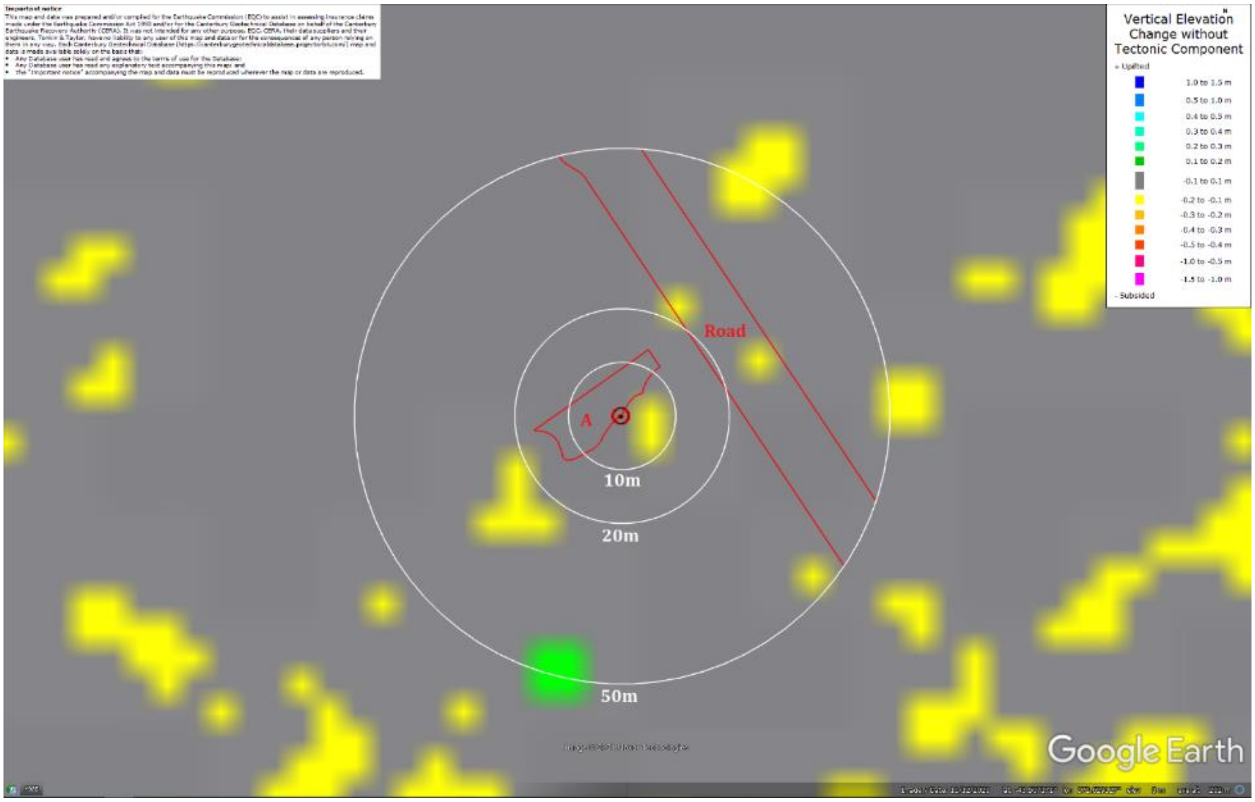

Figure 29: Ground surface subsidence without tectonic component for June 2011 Earthquake according to the LiDAR DEM.

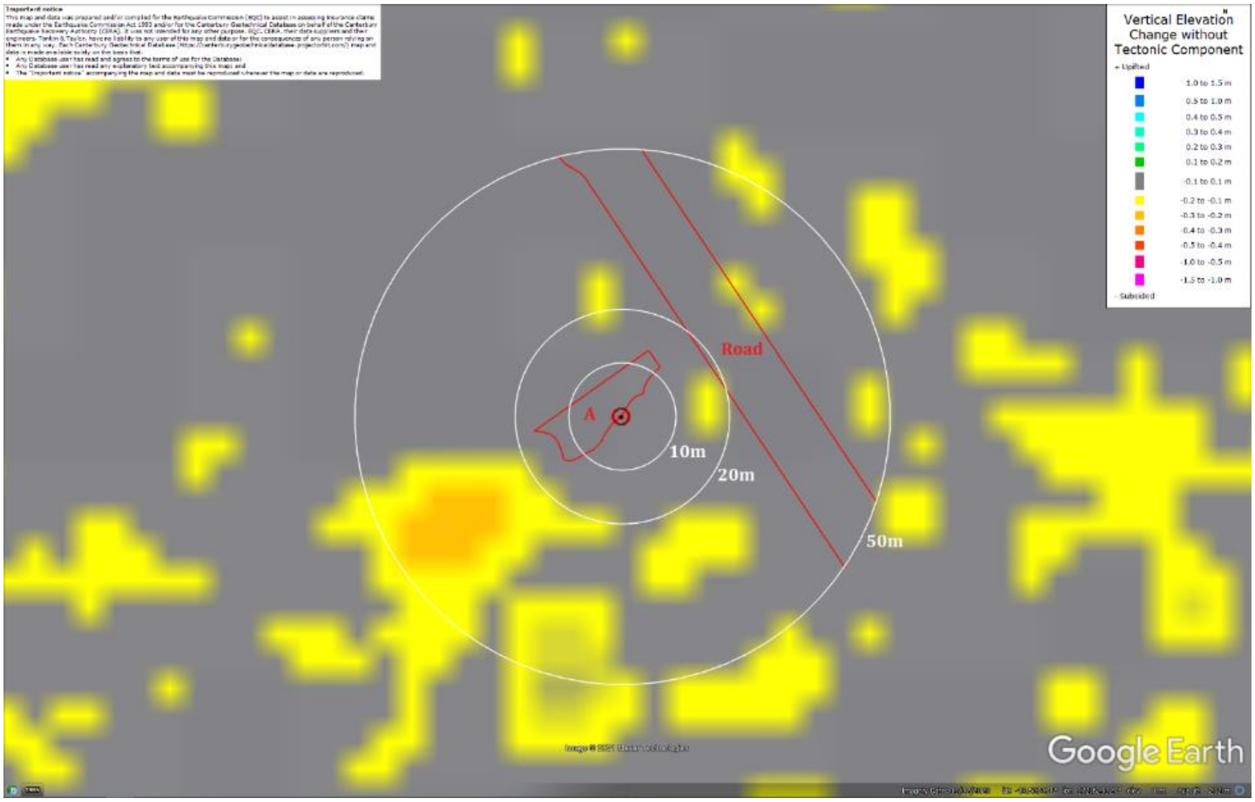

Figure 30: Ground surface subsidence without tectonic component for Dec 2011 Earthquake according to the LiDAR DEM.

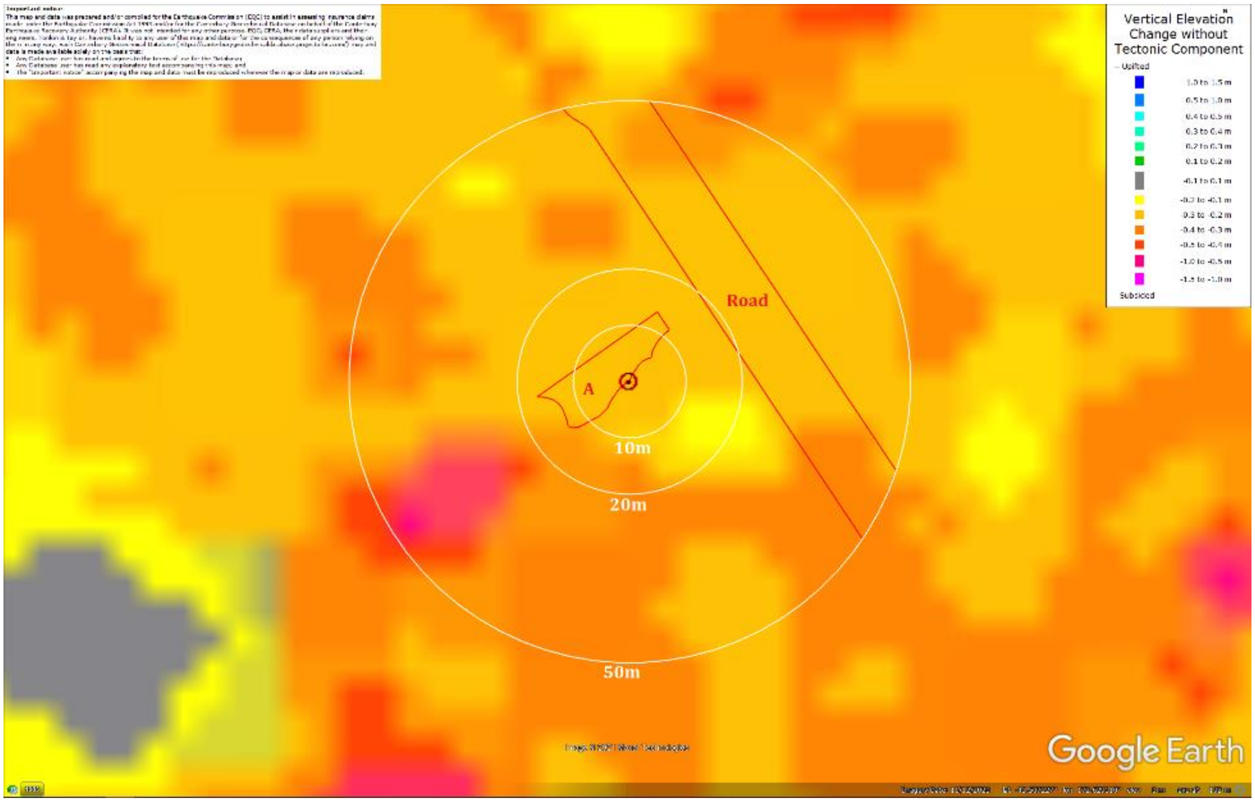

Figure 31: Ground surface subsidence without tectonic component for Canterbury Earthquake Sequence according to the LiDAR DEM.

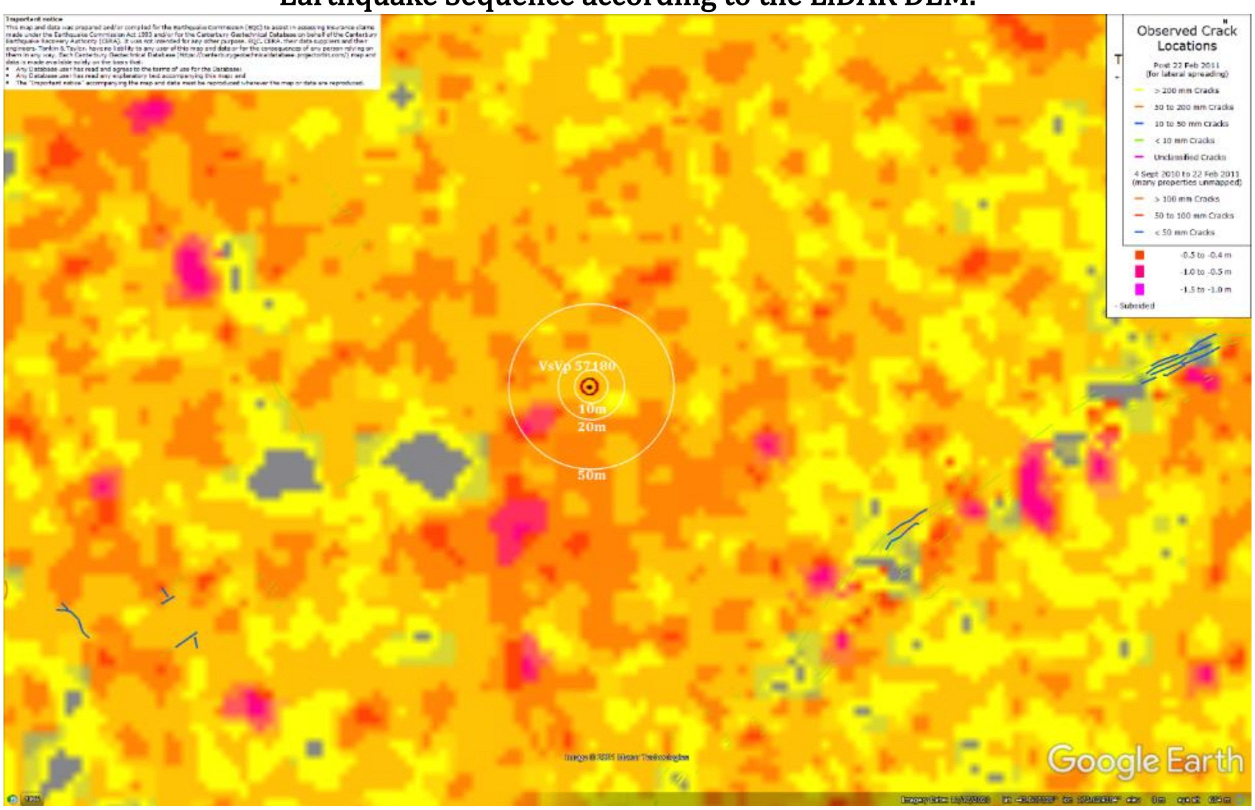

Figure 32: No lateral spreading for Canterbury Earthquake Sequence.

Figure 33: Vertical tectonic movements for Sep 2010 Earthquake.

Figure 34: Vertical tectonic movements for Feb 2011 Earthquake.

Figure 35: Vertical tectonic movements for June 2011 Earthquake.

Figure 36: Vertical tectonic movements for Dec 2011 Earthquake.

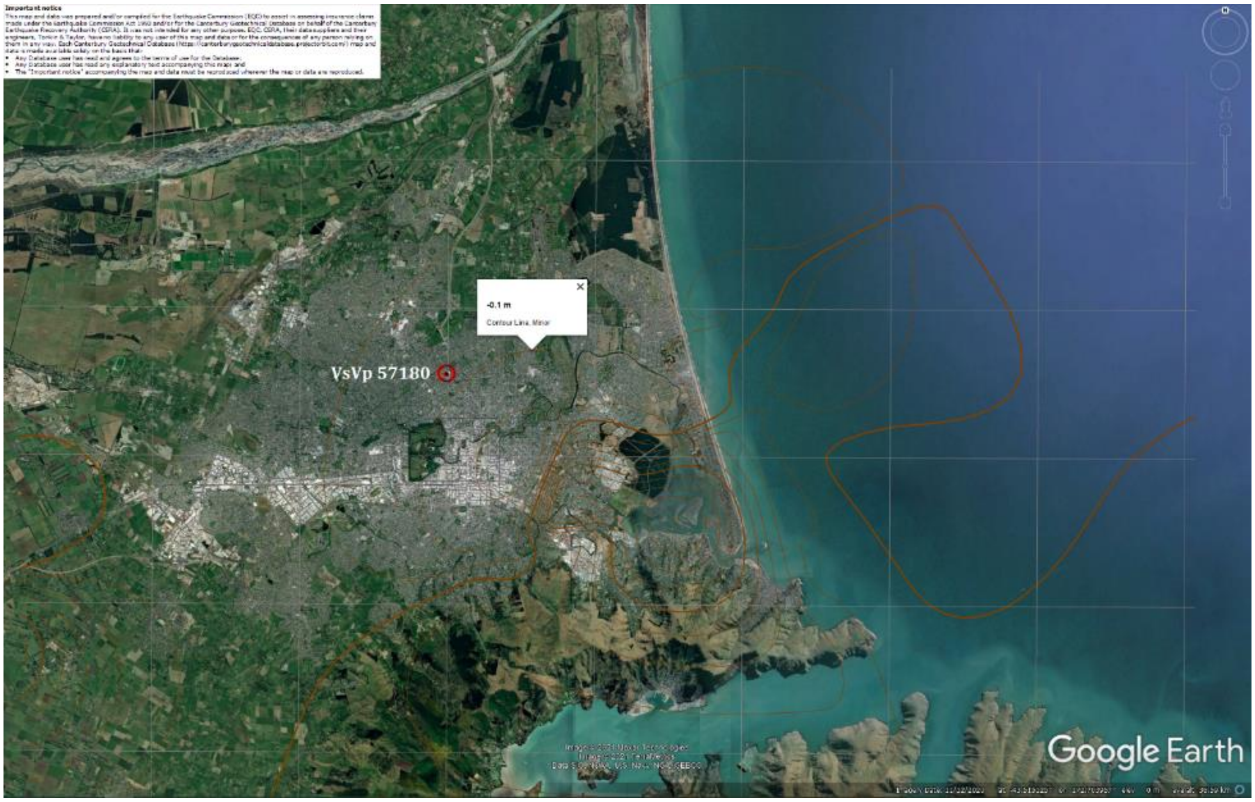

Figure 37: Vertical tectonic movements for Canterbury Earthquake Sequence.

Figure 38: Aerial photograph showing the ejecta outline at the site for Feb-11 EQ.

Figure 39: Aerial photograph acquired on 14-15 Jun 2011 showing the ejecta outline at the site for Jun-11 EQ.

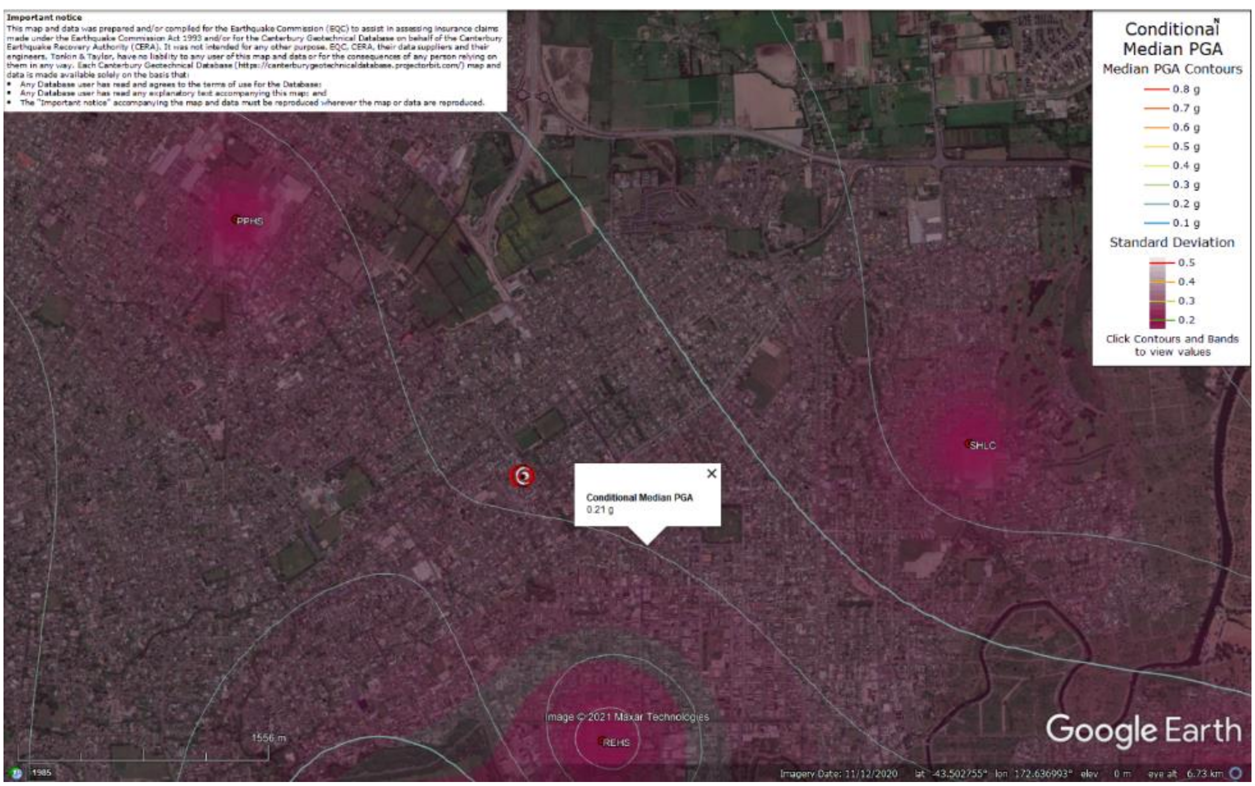

Figure 40: PGA for Sep-10 EQ (st. dev. = 0.300-0.325 ln units).

Figure 41: PGA for Feb-11 EQ (st. dev. = 0.350-0.375 ln units).

Figure 42: PGA for Jun-11 EQ (st. dev. = 0.350-0.375 ln units).

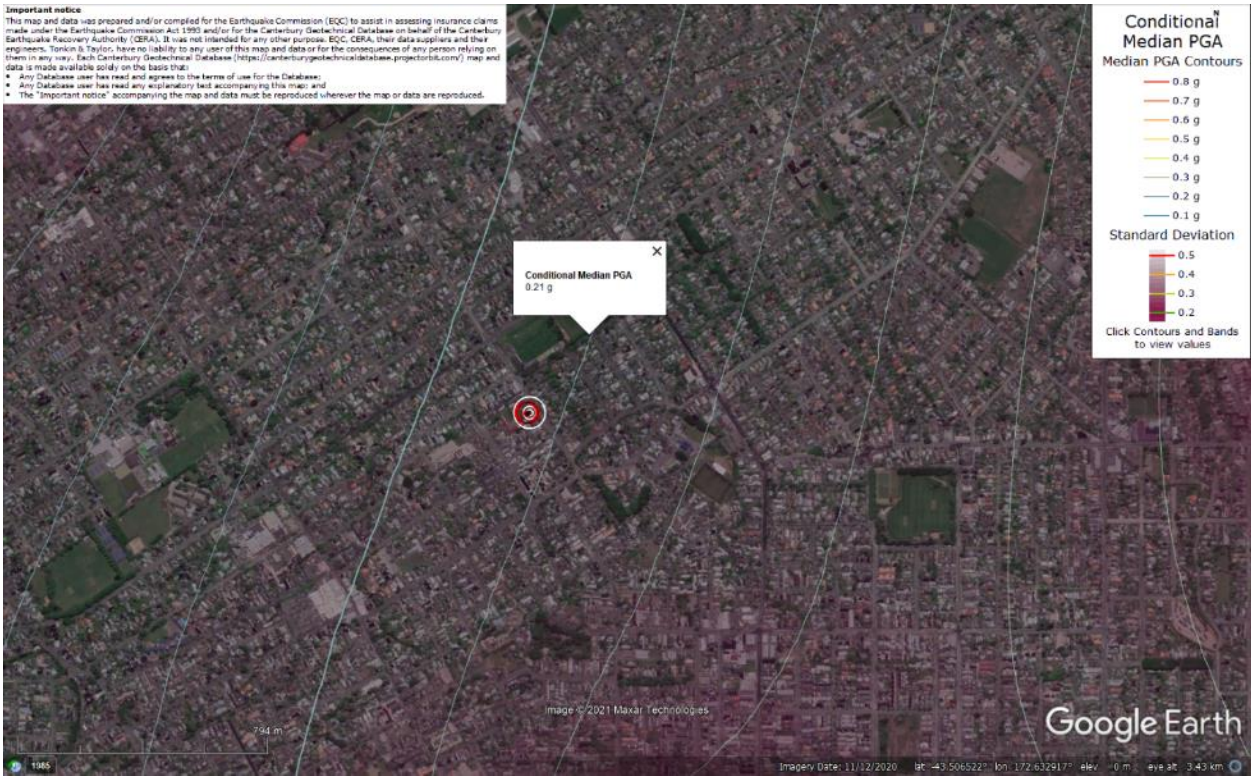

Figure 43: PGA for Dec-11 EQ (st. dev. = 0.350-0.400 ln units).

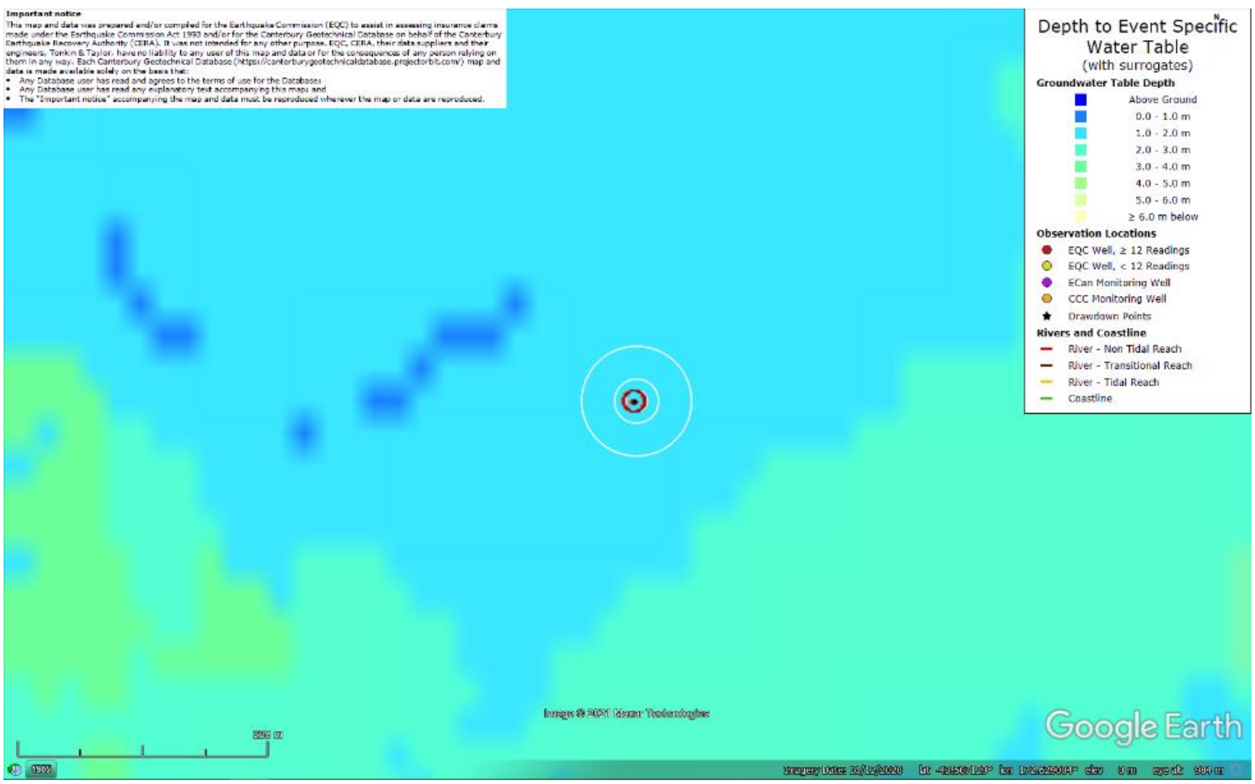

Figure 44: Depth to groundwater table for Sep-10 EQ.

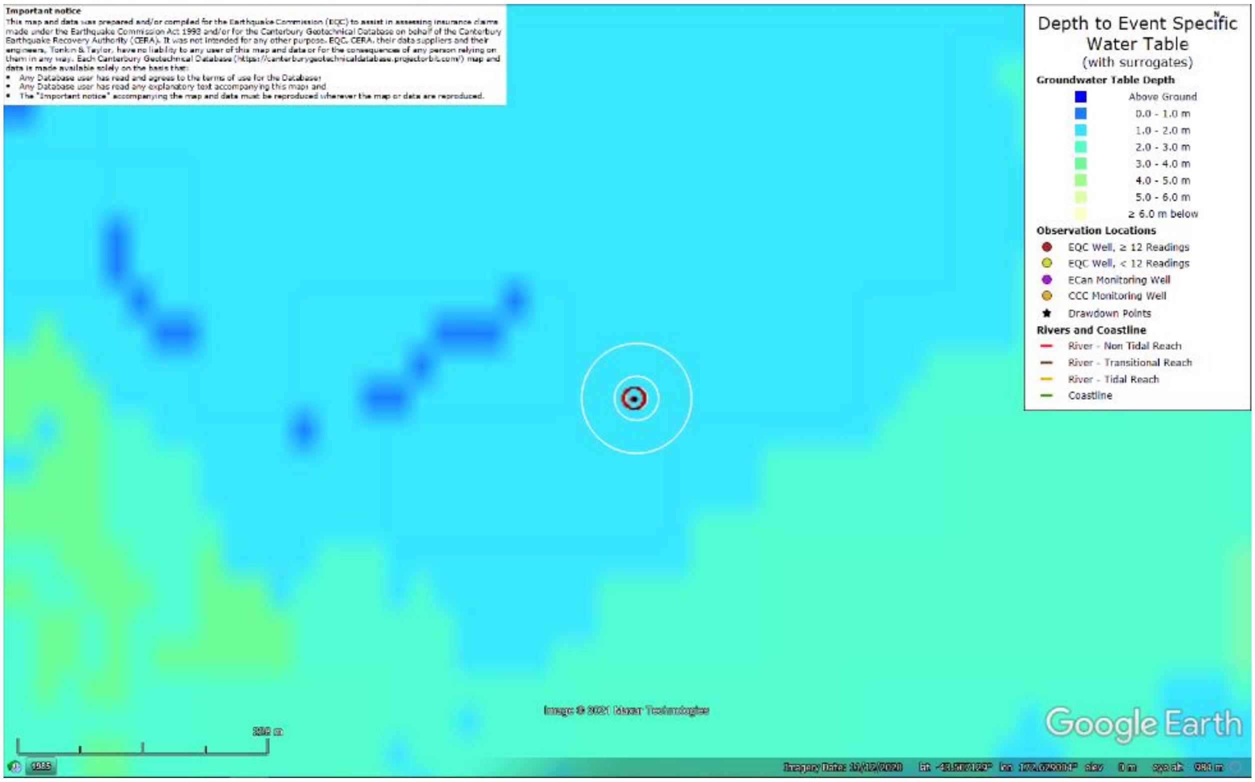

Figure 45: Depth to groundwater table for Feb-11 EQ.

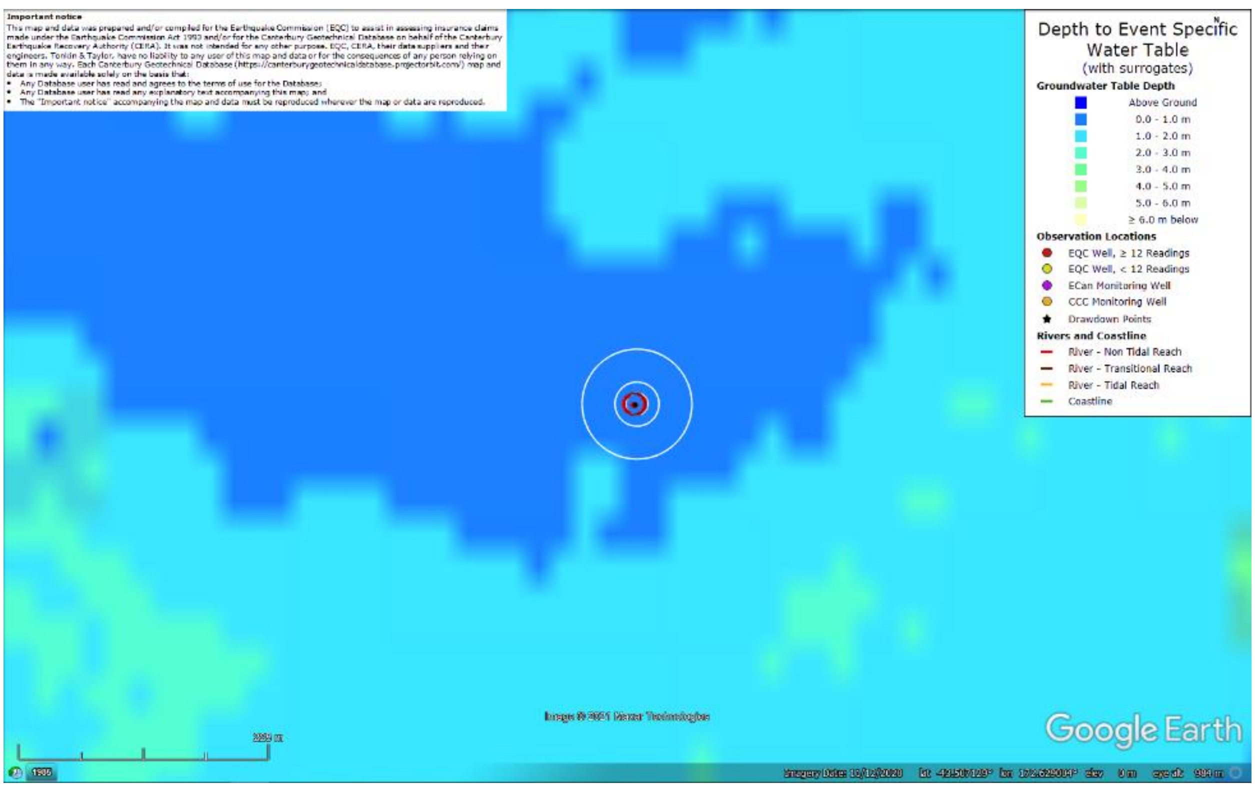

Figure 46: Depth to groundwater table for Jun-11 EQ.

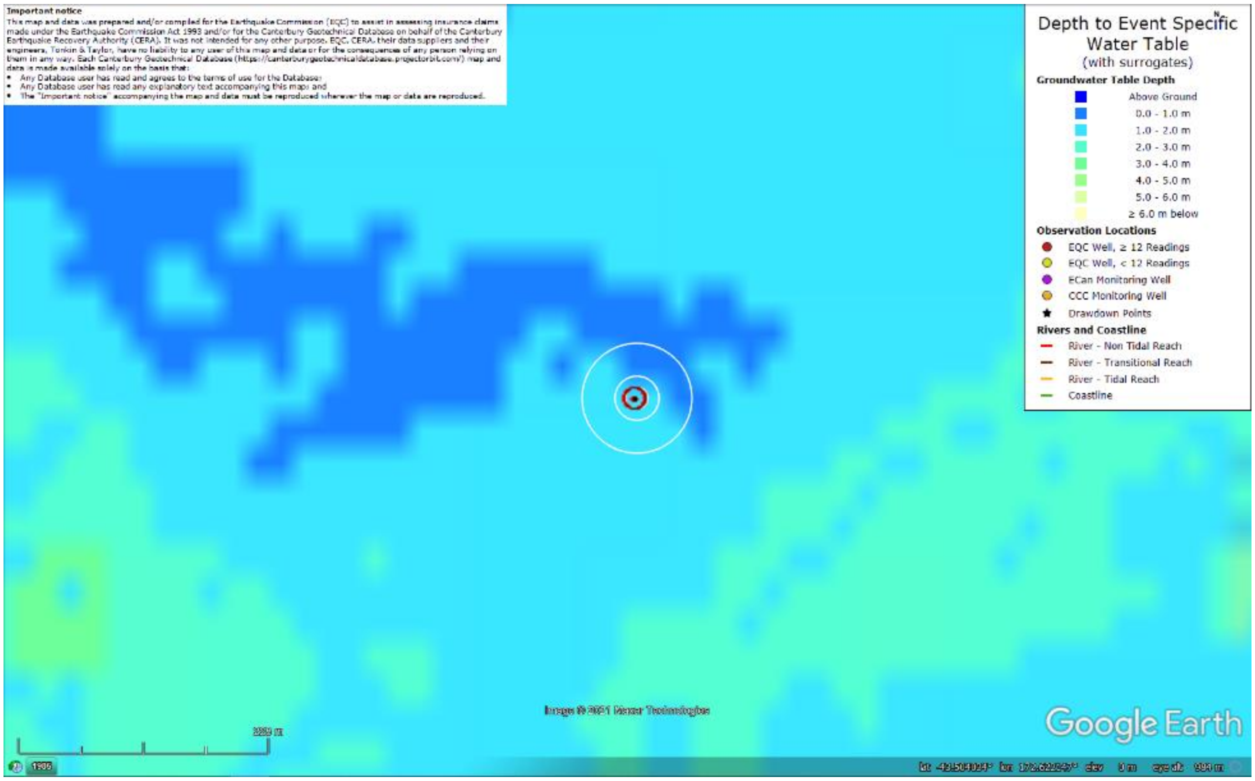

Figure 47: Depth to groundwater table for Dec-11 EQ.

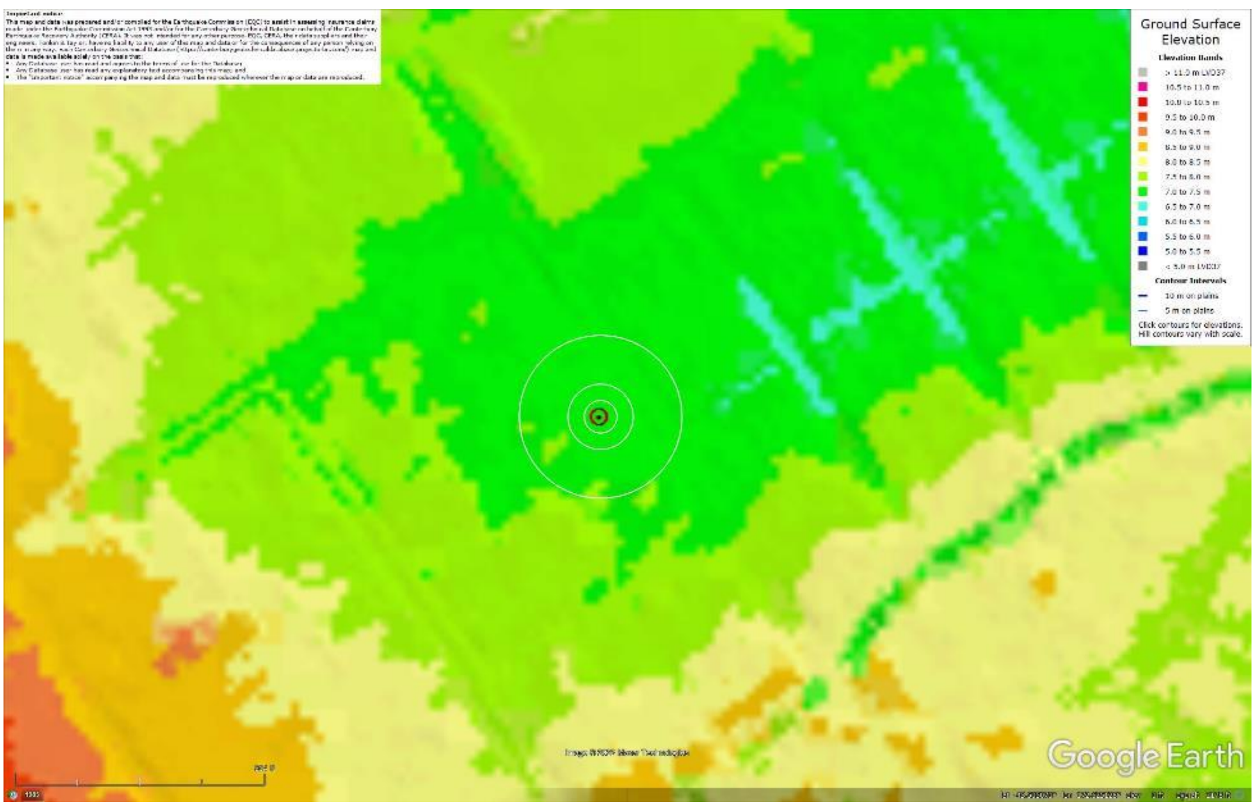

Figure 48: Ground surface elevation according to the Sep-11 LiDAR survey.

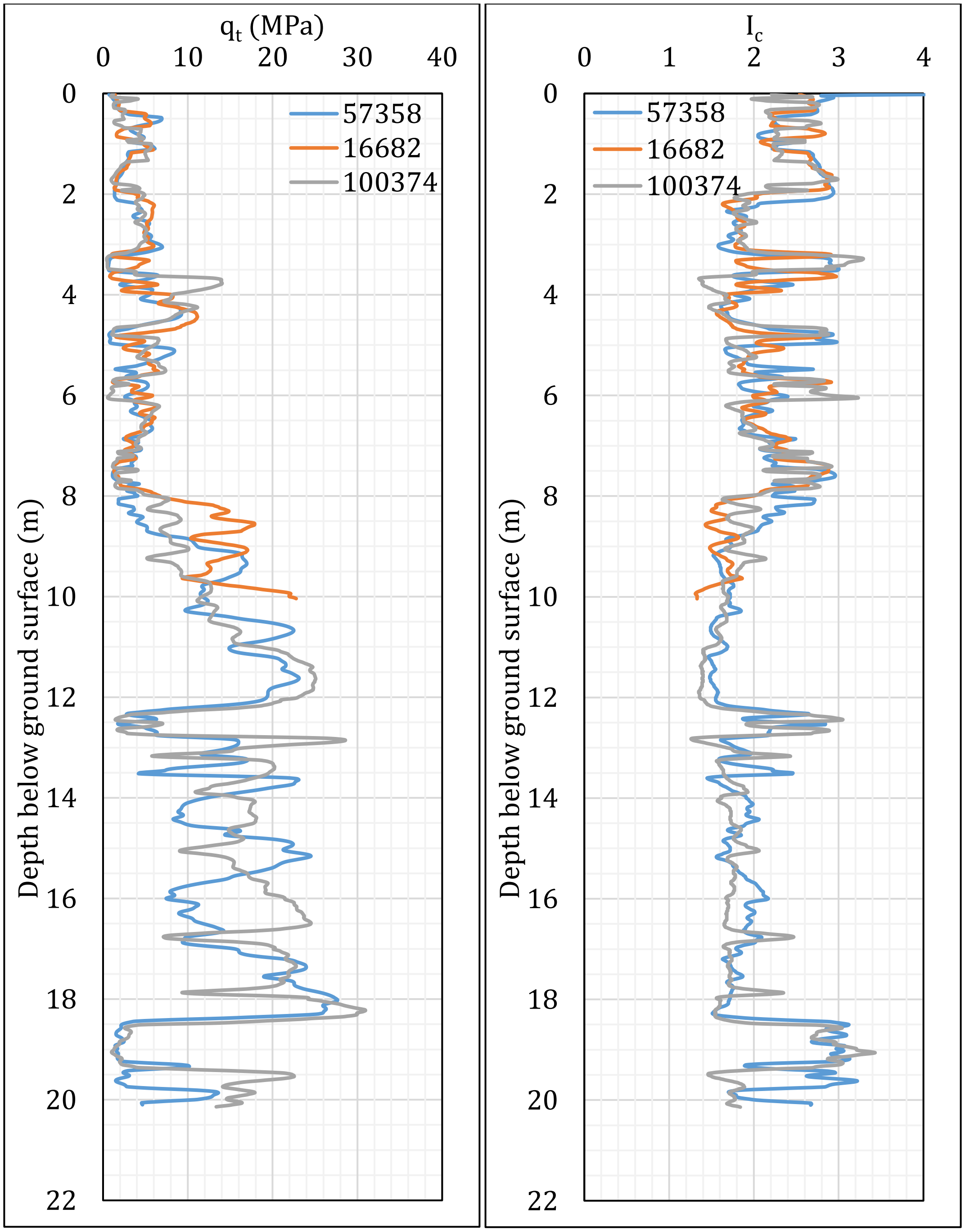

Figure 49: q_t and I_c profiles.

Note 6: The selection of CPTs for the area considered for settlement assessment (Figure 1) is based on the proximity of the CPTs to the considered areas. In accordance with that, the following table shows CPTs that were used for the volumetric settlement analysis in *Cliq v.3.0.3.2*, a CPT soil liquefaction software developed by GeoLogismiki. (The average volumetric settlements were reported in Table 8.)

Table 12: CPT profiles used in volumetric settlement analysis for areas selected for settlement assessment.

CPT ID No.	Patch A (10-, 20-, and 50-m buffers)	Road (50-m buffer)
57358 (56736)	✓	
16682		✓
100374 (104266)		✓

Note: CPT 57358 was used to compute the volumetric settlement for CPT 16682 for a depth range from 10 m to 20 m.

Table 13: CPT-based results.

		CPT ID			
EQ Event	Parameter	57358	16682	100374	$\Delta_{CPT16684}$
Sep-10	S_{V1D} (mm)	99	49	68	21
	LSN	15	9	11	1
	LPI	4	2	3	0
	LPI_{ish}	1	1	0	--
	$D_{FS<1}$ (m)	4.98	5.22	4.81	--
Feb-11	S_{V1D} (mm)	163	94	125	33
	LSN	28	20	22	3
	LPI	15	9	11	1
	LPI_{ish}	1	0	2	--
	$D_{FS<1}$ (m)	2.28	2.68	2.04	--
Jun-11	S_{V1D} (mm)	62	32	40	7
	LSN	11	7	7	1
	LPI	2	1	1	0
	LPI_{ish}	0	0	0	--
	$D_{FS<1}$ (m)	5.5	6.76	6.09	--
Dec-11	S_{V1D} (mm)	67	35	42	9
	LSN	11	7	7	1
	LPI	2	1	1	0
	LPI_{ish}	0	0	1	--
	$D_{FS<1}$ (m)	5.5	6.76	6.09	--

Notes: $D_{FS<1}$ = Depth to the first liquefiable layer (FS_L<1) that is at least 200-mm thick, as determined by the Boulanger and Idriss (2016) liquefaction-triggering procedure (P_L=50%, C_{FC}=0.13, and $I_{c,cutoff}$ =2.6), and exported from *Cliq v.3.0.3.2*; undet. = the specified soil layer was not detected; indicates the amount of S_{V1D}, LSN, and LPI added to CPT 16682 due to the shallow penetration depth.

Note 7: Based on the borehole log (BH 57223, Figure 1), the groundwater table is at a depth of 2.1 m below the ground surface. The soil profile consists of (1) organic silt, OL, as topsoil to a depth of 0.55 m, (2) silt, ML, the Yaldhurst member of the Springston formation, to a depth of 2.7 m, (3) fine sand, SP, the Yaldhurst member of the Springston formation, to a depth of 3.25 m, (4) silt, ML, the Yaldhurst member of the Springston formation, to a depth of 4.4 m, (5) fine sand, SP, the Yaldhurst member of the Springston formation, to a depth of 4.75 m, (6) silt, ML, the Yaldhurst member of the Springston formation, to a depth of 5.8 m, (7) silty fine sand, SM, the Yaldhurst member of the Springston formation, to a depth of 7.0 m, (8) silt, ML, the Yaldhurst member of the Springston formation, to a depth of 8.45 m, and (9) fine to medium sand, SP, of the Christchurch formation, to a depth of 15.65 m (the end of the borehole). According to BH 1867, which is ~110 m to the NE from the center of the site, the SP layer continues to a depth of 20 m.

Note 8: The ejecta-induced free-field settlement provided in Table 11 is an areal average settlement due to ejecta, which is based on the total settlement assessment area, A_T (provided in Table 9 and repeated in Table 14). However, the considered area was not always covered completely with ejecta; thus, it is important to provide the localized ejecta-induced settlement, too. The localized settlement due to ejecta is estimated using photographic evidence only as

$$S_{E,P\_localized} = \frac{V_E}{A_E}$$

where V_E is the total volume of ejecta within A_T and A_E is the total coverage area of ejecta within A_T. Please note that the areal ejecta-induced settlement provided in Table 14 as S_{E,P_areal} is the same as $S_{E,P}$ in Table 11, which was estimated as

$$S_{E,P\_areal} = S_{E,P} = \frac{V_E}{A_T}$$

where V_E is the total volume of ejecta within A_T and A_T is the total settlement assessment area.

Table 14a: Areal and localized ejecta-induced settlement estimates for Patch A (20-m and 50-m buffers) based on photographic evidence.

Earthquake Event	A_T (m²)	A_E (m²)	V_E (m³)	S_{E,P_areal} (mm)	$S_{E,P\_localized}$ (mm)
Sep-10	168	0	0	0	0
Feb-11	168	19.2	0.6-1.0	5±5	40±10
Jun-11	168	13.3	0.3-0.5	<5	30±10
Dec-11	168	0	0	0	0

Notes: S_{E,P_areal} = $S_{E,P}$ reported in Table 11 = areal ejecta-induced settlement; $S_{E,P\_localized}$ = localized ejecta-induced settlement; A_T = total settlement assessment area; V_E = total volume of ejecta within A_T; A_E = total area of ejecta within A_T; The estimates of both areal and localized ejecta-induced settlement are rounded to the nearest 5; Final plus/minus values are also rounded to the nearest 5.

Table 14b: Areal and localized ejecta-induced settlement estimates for Road (50-m buffer) based on photographic evidence.

Earthquake Event	A_T (m^2)	A_E (m^2)	V_E (m^3)	S_{E,P_areal} (mm)	$S_{E,P\_localized}$ (mm)
Sep-10	1027	0	0	0	0
Feb-11	950	474	1.3-2.6	<5	5±5
Jun-11	916	916	1.7-7.3	5±5	5±5
Dec-11	1027	0	0	0	0

Notes: S_{E,P_areal} = $S_{E,P}$ reported in Table 11 = areal ejecta-induced settlement; $S_{E,P\_localized}$ = localized ejecta-induced settlement; A_T = total settlement assessment area; V_E = total volume of ejecta within A_T; A_E = total area of ejecta within A_T; The estimates of both areal and localized ejecta-induced settlement are rounded to the nearest 5; Final plus/minus values are also rounded to the nearest 5.

Summary 2:

- **The best estimate of the localized ejecta-induced free-field ground settlement at the St. Albans Catholic School site for the SEP 2010, FEB 2011, JUN 2011, and DEC 2011 earthquake is 0 mm, 40±10 mm, 30±10 mm, and 0 mm, respectively.**
- **The best estimate of the localized ejecta-induced free-field settlement of the road at the St. Albans Catholic School site for the SEP 2010, FEB 2011, JUN 2011, and DEC 2011 earthquake is 0 mm, 5±5 mm, 5±5 mm, and 0 mm, respectively.**